

# Analyst

Accepted Manuscript



This is an *Accepted Manuscript*, which has been through the Royal Society of Chemistry peer review process and has been accepted for publication.

*Accepted Manuscripts* are published online shortly after acceptance, before technical editing, formatting and proof reading. Using this free service, authors can make their results available to the community, in citable form, before we publish the edited article. We will replace this *Accepted Manuscript* with the edited and formatted *Advance Article* as soon as it is available.

You can find more information about *Accepted Manuscripts* in the [Information for Authors](#).

Please note that technical editing may introduce minor changes to the text and/or graphics, which may alter content. The journal's standard [Terms & Conditions](#) and the [Ethical guidelines](#) still apply. In no event shall the Royal Society of Chemistry be held responsible for any errors or omissions in this *Accepted Manuscript* or any consequences arising from the use of any information it contains.

# A colorimetric and smartphone readable method for Uracil-DNA glycosylase detection based on the target-triggered formation of G-quadruplex

Huaijun Nie, Wei Wang, Wang Li,\* Zhou Nie, Shouzhao Yao

*State Key Laboratory of Chemo/Biosensing and Chemometrics, College of Chemistry and Chemical Engineering, Hunan University, Changsha, 410082, P. R. China.*

*Fax: +86-731-88821848; Tel: +86-731-88821626;*

*E-mail: wli@hnu.edu.cn (W. Li)*

## Abstract

A simple, visible and smartphone readable strategy for sensitive detection of uracil DNA glycosylase (UDG) activity, which is based on UDG-catalyzed removal of uracil bases inducing the formation of G-quadruplex/cofactor complex. Guanine-rich DNA probe can form a special G-quadruplex structure with hemin to display peroxidase activity to catalyze the H<sub>2</sub>O<sub>2</sub>-mediated oxidation of ABTS<sup>2-</sup> to the colored ABTS<sup>•-</sup>, providing a visible signal for UDG detection. The proposed sensing platform exhibits a good linear response to UDG concentration ranging from 0.008 to 0.2 U/mL with a low detection limit of 0.008 U/mL. Based on the chromatics theory, we can directly read out the color value using a smartphone App to reflect the content of UDG with high resolution, providing a new vision for the portable assay strategy. Furthermore, the utility of this method for screening potential UDG inhibitors was also demonstrated.

## Introduction

Cells endure incessant DNA base damage which threatens their viability and genomic stability.<sup>1</sup> DNA damage is suggested to contribute to cell aging through their ability to mediate cellular dysfunction.<sup>2</sup> If these bases lesion remains unrepaired, it will lead to gene instabilities during the encoding of genetic information in DNA and may increase cancer risk.<sup>3</sup> DNA base excision repair (BER) is the major means to eliminate those damage in cell.<sup>4</sup> As a key BER glycosylase, Uracil-DNA glycosylase (UDG) can remove the undesired uracil from DNA strand.<sup>1,5</sup> Since the BER process plays a very important role in maintaining genetic integrity and relate diseases, developing convenient UDG detecting method of high performing is significant in multiple respects, such as the mechanism studies of the UDG, and anti-cancer drug candidates screening.<sup>6,7</sup>

Traditional methods for UDG assay mainly focus on radioactive labeling,<sup>8</sup> gel-electrophoresis<sup>9</sup> and mass spectrometry.<sup>10</sup> However, these methods are known to be time consuming, operation tedious, indirect, need sophisticated instruments, and always fail to meet the desirable detection limit. Considering that, many scientists devote to improve the UDG detection method, most of their work focus on fluorescent label methods,<sup>11-13</sup> also some devote themselves to electrochemical sensing<sup>14</sup> or

1  
2  
3  
4  
5  
6  
7  
8  
9  
10  
11  
12  
13  
14  
15  
16  
17  
18  
19  
20  
21  
22  
23  
24  
25  
26  
27  
28  
29  
30  
31  
32  
33  
34  
35  
36  
37  
38  
39  
40  
41  
42  
43  
44  
45  
46  
47  
48  
49  
50  
51  
52  
53  
54  
55  
56  
57  
58  
59  
60

UV-Vis platform.<sup>15</sup> Although those approaches have significant improvement in the detection limit, but still some limitations exist. For example, sophisticated instruments are still in need, many of them rely on tedious and costly fluorophore modification,<sup>11-13</sup> and some even need other enzymes such as nicking enzyme,<sup>15</sup> polymerase<sup>11</sup> or hydrolase,<sup>16</sup> it is always time-consuming, complicated and susceptible. What's more, rare method is qualified to cater to the development of the ubiquitous portable electronics in the modern society, and most of the existing assay methods are short of humanistic concern. Therefore, in view of these drawbacks, a humanized strategy should be developed to connect the science work with ordinary life. So a low cost, simple and easy to operate assay of UDG is in demand.

Exploiting a simple, visualized and portable strategy to achieve effective analysis of UDG activity is our original purpose. G-quadruplexes DNA probe is a good choice for its easy synthesis, highly adaptable and super-sensitive. Guanine-rich DNA strand can form a kind of four-stranded structure known as G-quadruplex, which can bind to some small molecules with high affinities.<sup>17</sup> Once G-quadruplex bind with hemin (an anionic iron (III) porphyrin), it can exhibit peroxidase catalytic activity. G-quadruplex-hemin complex named DNAzyme can catalyze the oxidation of 2,2-azino-bis(3-ethylbenzothiazoline)-6-sulfonate disodium salt (ABTS<sup>2-</sup>) by H<sub>2</sub>O<sub>2</sub> to produce the visual colored ABTS•<sup>-</sup>.<sup>18</sup> Based on the chromatics theory, image analysis of enzyme activity using RGB (Red-Green-Blue) image profiling is a novel technique.<sup>19-21</sup> Portable smartphone may provide more accurate data for UDG assay. In addition, G-quadruplexe can also interact with some water-soluble fluorogenic dyes such as Thioflavin T (ThT) with a high emission enhancement in the visible region.<sup>22</sup> Regard of these properties of G-quadruplexes DNA complex, we decide to develop a label-free visible colorimetric and fluorescent UDG detection method based on G-quadruplexes, expecting to achieve an outstanding performance during UDG detection.

## Experiment section

### Materials and Measurements.

4-(2-hydroxyethyl) piperazine-1-ethanesulfonic acid sodium salt (Hepes), ABTS<sup>2-</sup>, hemin, 3,6-dimethyl-2-(4-dimethylaminophenyl) benzo-thiazolium cation (Thioflavin T ThT), and DNA oligonucleotides are purchased from Shanghai Sangon Biological Engineering Technology & Services Co., Ltd (Shanghai, China). UDG and Uracil DNA glycosylase inhibitor (UGI) are purchased from New England Biolabs (USA). Other chemicals are of analytical reagent grade and used without further purification. Ultrapure water (18.25 MΩ cm) is obtained from a Millipore filtration system and used throughout. UV-Vis absorption spectra are obtained on a BECKMAN DU-800 spectrophotometer. Fluorescence spectra are measured on a QuantaMaster<sup>TM</sup> fluorescence spectrophotometer, PTI (Canada).

The DNA sequences (5'-3') used in the experiment are as follows:

La1: CTGCTGAGGGATGGGUGGGTAGGGATGTTCAG

La2: CTGCTGAGGGAUGGGTGGGUAGGGATGTTCAG

Lb1: GAACATCCCTACCCACCCATCCCTCAG

Lb2: AACATCCCTACCCACCCATCCCTCAG

Lb3: AACATCCCTACCCACCCATCCCTCA

Lb4: ACATCCCTACCCACCCATCCCTCA

Lb5: ACATCCCTACCCACCCATCCCTC

Lb6: CATCCCTACCCACCCATCCCTC

### Assay of UDG activities

The enzyme reaction system contain about 250 nM ssDNA La, 300 nM ssDNA Lb, UDG reaction buffer (20 mM Tris-HCl, pH = 8.2, 10 mM EDTA, 100 mM NaCl) and a series of UDG with different concentration, the total volume of the reaction system is 50  $\mu$ L. The sample is incubated at 37  $^{\circ}$ C for 1 hour. The signal generation experiment of hemin-G-quadruplex complexes: 1  $\mu$ L hemin (10  $\mu$ M) and 20  $\mu$ L UDG reaction solution were introduced into 59  $\mu$ L DNAzyme buffer (200 mM NaCl, 20 mM KCl, 25mM hepes, pH = 5.3, 0.01% (v/v) Triton X-100), 15 minutes later, 10  $\mu$ L of 20 mM ABTS<sup>2-</sup> and 10  $\mu$ L of 20 mM H<sub>2</sub>O<sub>2</sub> were added to initiate the catalytic oxidation of ABTS<sup>2-</sup>. The UV-vis absorption spectra were obtained at 415 nm at room temperature.

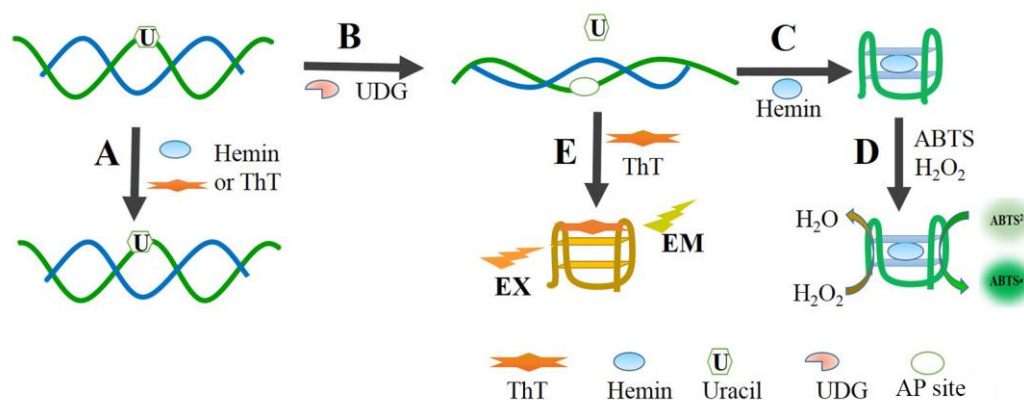
### Assessment of UDG activity through fluorescence detection.

For fluorescence detection, after the UDG reaction, 3  $\mu$ L of 100  $\mu$ M ThT, 15  $\mu$ L of 200 mM Tris-HCl buffer (pH = 7.2), 10  $\mu$ L of 100mM KCl, and 22  $\mu$ L H<sub>2</sub>O were added into the sample. Twenty minutes later, the emission spectra were monitored from 445 to 550 nm with excitation at 425 nm.

### PAGE (20%) for the heteroduplex unwinding demonstration

For the 20% Polyacrylamide gel electrophoresis (PAGE) analysis of the heteroduplex unwinding, the process of uracil excision by UDG was conducted as the same as aforementioned except concentration of La<sub>1</sub> and Lb<sub>4</sub> were 1.5  $\mu$ M, and the UDG concentration here is 10 U/mL. The samples were loaded into a 20% polyacrylamide gel and the electrophoresis was carried in tris-borate-EDTA (TBE) buffer (90 mM Tris, 90 mM boric acid, 10 mM EDTA, and 12.5 mM MgCl<sub>2</sub> pH 8.0) at 90 V for 3 h. The gel was stained by SYBR Green II for 20 min and scanned by a ChemiDoc™ MP System (Bio-Rad).

## Results and Discussions



**Scheme 1** Schematic diagram the principle of UDG activity assay.

The proposed mechanism of the UDG activity assay is outlined in Scheme 1. La, the guanine-rich and uracil containing DNA strand, is initially hybridized with a partially complementary chain to form a duplex substrate in the absent of UDG (path A). Once UDG exists, the uracil will be cut off from the guanine-rich strand La, thereby generating apurinic/apyrimidinic (AP) sites on La. The produced AP sites will significantly decrease the stability of duplex substrate and loosen the hybrid duplex (path B). Then the cofactors in the system induce the guanine-rich strand to unwind from the hybrid strand and to fold into a G-quadruplexe conformation, thus the signal generator formed. If the guanine-rich section couples with hemin, the complexes called DNAzyme can exhibit efficient catalytic activity towards the  $\text{H}_2\text{O}_2$ -mediated oxidation of  $\text{ABTS}^{2-}$ , producing the colored radical ion  $\text{ABTS}^{\bullet-}$  (path C and D). Therefore, taking the advantage of the present strategy, the UDG activity can be easily monitored by naked-eye, smartphone App or UV-Vis spectroscopy.

UV-Vis spectroscopic measurements and PAGE analysis for samples under different conditions were carried out firstly to verify the feasibility of the proposed strategy. As shown in Fig.1A, the single strand of La1 without a complementary strand exhibits the highest catalytic activity when combined with hemin (Fig. 1A (a)). When La1 hybridizes with its complementary strand, a weakly catalytic activity exhibits (c), representing that the La1 is prohibited to combine with hemin and can't fold into the active G-quadruplex/hemin HRP-mimicking DNAzyme structure. When the sample is treated with UDG, high catalytic activity reappears (b), indicating that the duplex is destroyed. Corresponding colorimetric detections are shown in inserted Fig.1A. Therefore, the DNAzyme system presents excellent response to the UDG. For further investigation of the mechanism of our method, the hydrolysis events by UDG are probed by electrophoresis analysis with PAGE. The gel image of Fig.1B demonstrates that after the interaction with UDG, Lb4 separates from La1 (lane 3 and lane 4). As a whole, all the aforementioned results demonstrate that it is rational to probe hydrolysis by UDG, providing a solid foundation for the following experiments.

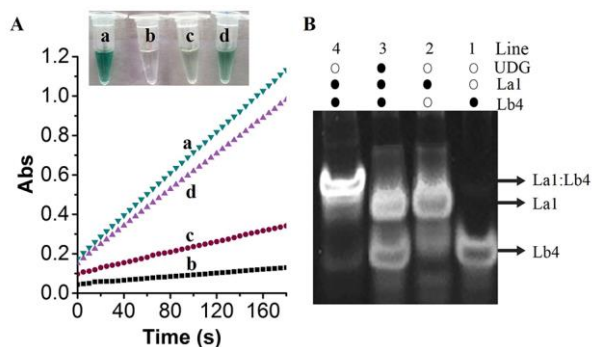


**Fig.1** (A) UV-Vis absorption spectra and photography (inset) to show the DNAzyme activity of hemin-generated G-quadruplexes in the ABTS<sup>2-</sup>-H<sub>2</sub>O<sub>2</sub> system. (a) La1; (b) Lb4; (c) La1 and Lb4 without UDG; (d) La1 and Lb4 with 2 U/mL UDG. (B) PAGE analysis of the dissociation of the double-stranded substrate. Line 1: Lb4; Line 2: La1; Line 3: La1 and Lb4 with 10 U/mL UDG; Line 4: La1 and Lb4 without UDG.

### Optimization of the experimental condition

At first, the length of hybridization chain (Lb) was optimized for the best analytical performance. La1 is a guanine-rich DNA strand that can be divided into two functional segments, with the guanine-rich motif in the middle as the signal generation part, and the tails at two terminals which provide extra binding sites for Lbs. In order to obtain a considerable signal change before and after the uracil treating, a series of Lbs with chain length ranging from 22 to 27 base pairs were designed. The diverse Lbs were applied to conduct a series of experiments respectively under the concentration of 2 U/mL UDG. Fig. 2A and Fig. 2B show that the signal of the absorbance increases orderly and melting temperature ( $T_m$ ) lower correspondingly as the length of Lb decrease, whether the samples were treated with or without UDG. Fig. 2A shows that when the hybridized base pairs decrease to some degree, all the heteroduplex unwinds as the uracil is cut off from the guanine-rich strand,  $\Delta Abs$  reaches a plateau value. In addition, the background signals increase rapidly as the hybridized base pairs decrease. We infer that La1 has two existent states when Lb exists, including hybridization with Lb and formation a G-quadruplex. With the chain length of Lb shortening, more La1 form G-quadruplex. When the uracil is excised from the heteroduplex, the hybrid duplex is unstable and the  $T_m$  is decreasing, leading to more G-quadruplex formation and the  $\Delta Abs$  raises. After the optimization, Lb4 with the biggest signal-noise ratio (signal/background) was chosen to conduct the next experiments.



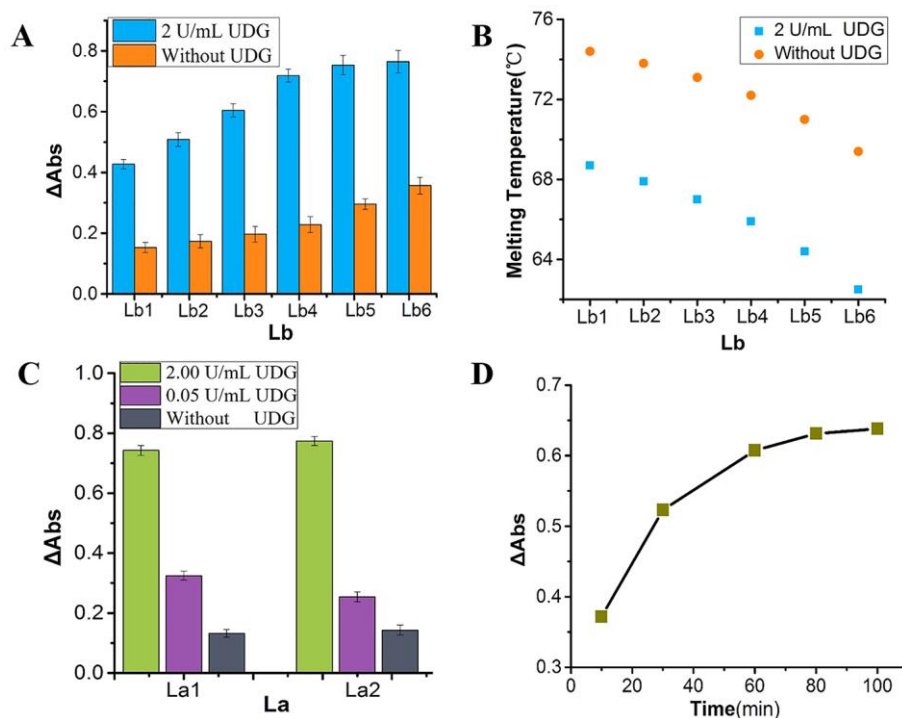


**Fig. 2** (A) UV-Vis absorbance changes at 415 nm of La1 hybridizing with different length of Lbs. (The blue bars: treated with 2 U/mL UDG; the orange bars: without UDG). (B) The melting temperature of the LA1 hybridizing with different length of Lbs. (The blue dots: treated with 2 U/mL UDG; the orange dots: without UDG). (C) Absorbance change of La1 or La2 hybridized with Lb4. (The green bars: treated with 2 U/mL UDG, the purple bars: treated with 0.05 U/mL UDG, the gray bars: without UDG). (D) The dependence of absorbance change on the UDG reaction time with 0.2 U/mL UDG.

For further optimization of the DNA strands, the number of uracil on the La strand has been investigated (Fig. 2B). Almost all the reported UDG detection methods require at least two uracils in the substrate DNA probes.<sup>14,15,23-25</sup> So we want to figure out whether double uracils in the substrate DNA are still the dominant choice compared with a single uracil. On the basis of La1, another DNA strand La2, which consists with two uracils, was designed. A series of experiments were carried respectively to investigate the discrepancy of La1 and La2. The results in Fig. 2B shows that when the UDG is excessive (2 U/mL), La2 has a slightly better performance compared with La1. Because in this case, the duplex with double AP sites is less steady than that with one AP site. However, at low concentration of UDG (0.05 U/mL), La1 is the superior choice. Since UDG excise the uracil on DNA strand randomly, it may remove the uracils on the same La2 strand, but leave lots of un-excised DNA. Therefore, the performance of La with a sole uracil is superior compared with two uracils in it. In addition, it is noticeable that the uracil is placed in the La strand elaborately, and this behavior can effectively avoid the loss of sensitivity caused by artificially operation.

Furthermore, the reaction time of UDG is optimized. Generally, for the detection time, the shorter the better, at the same time, the sensitivity should also be considered.

Therefore, different detection time of 10 min, 30 min, 60 min, 80 min and 100 min were investigated under the concentration of 0.2 U/mL UDG. Fig. 2C shows the absorbance changes observed upon different UDG reaction time. The increase of UDG reaction time leads to a sharp increase of the absorbance values until 60 minutes. With a comprehensive consideration of the shorter detection time and the sensitivity of the sensor, the time of 60 minutes was chosen as UDG reaction time.

### Detection of UDG activity

Based on all the pre-optimized condition, the quantitative detection of UDG activity was first carried out on the hemin-G-quadruplex platform. As the concentration of UDG increased, more La1 break away from the heteroduplex and more G4-DNAzyme formed with hemin, causing the increase of production of radical ion ABTS•-. Fig. 3 shows the kinetic absorbance changes at 415 nm upon different concentrations of UDG. A good linear response was observed in the concentration of UDG ranging from 0.008 to 0.2 U/mL, with a linear equation of  $\Delta Abs = 2.32C_{UDG} + 0.15$ . The detection limit of this non-enzyme assisted strategy is about 0.008 U/mL, which is lower than the method developed by Li's group based on nicking enzyme as signal circulator (0.02 U/mL);<sup>15</sup> somewhat higher than Yu's fluorescent-labeled strategy (0.0023 U/mL)<sup>11</sup> using roll circle amplification (RCA) as signal amplify system.

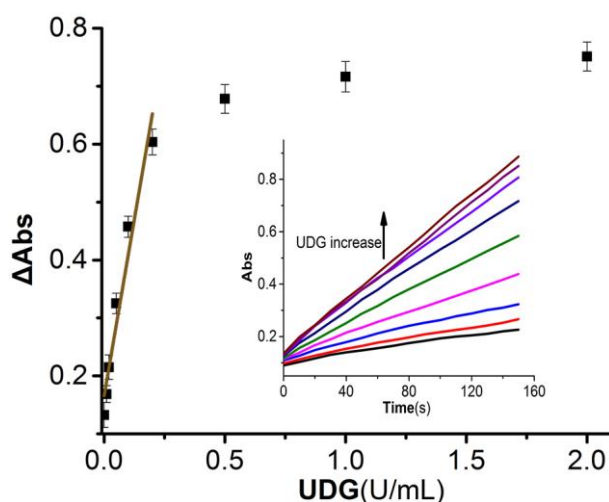


**Fig. 3** The absorbance change plotted as a function of the UDG concentration. The insert figure shows the changes of time-dependent absorbance at 415 nm *versus* different concentration of UDG.

In order to meet the developing trend of the analytic science in the “smartphone relied society”, we tried to run our whole detection system on a smartphone. With the development of the life science and electrical science and technology, mobile terminal will be the main type of personalization medical diagnosis devices in the future. Through a smartphone, people can monitor their body indices whenever and wherever possible, which will not only exist in the science fiction anymore. Chromatics theory indicates that every color is composited by three-primary colors (Red-Green-Blue, RGB), and RGB image profiling is a novelty technique in analytic chemistry.<sup>26,27</sup> We



wonder whether we can directly use the color value to reflect the content of our target. A new method of RGB analysis, using the smartphone as the one and all devices, is applied to sense the UDG activity. Instead of shifting the detection system into cuvette and detecting under the spectrophotometer, we add the solution into centrifuge tube and then an App is used to readout the RGB value. From the photograph taken by phone we can generalize that as the UDG concentration gradually increase, the green deepen correspondingly (Fig. 4B). As the color deepen, the value of green read by App decrease respectively. In order to simplify the computational model, the interaction among different colors was ignored, and only the value of green was explored and associated with the concentrations of UDG here. To diminish the stochastic error, five points were picked out from one tube and then an average were taken, and the data for different concentration of UDG was shown in Fig. 4C. It is remarkable that the resolution of a smartphone apparently overwhelms that of the naked-eye. The difference between these three samples in Fig. 4D can be resolved by smartphone facilely, however, it is difficult for naked-eye to distinguish. Therefore, the smartphone can provide a higher resolution than naked-eye. This novel method may provide a new angle of view for analytic science, and we firmly believe that it will be a major development tendency for biosensors in the future.

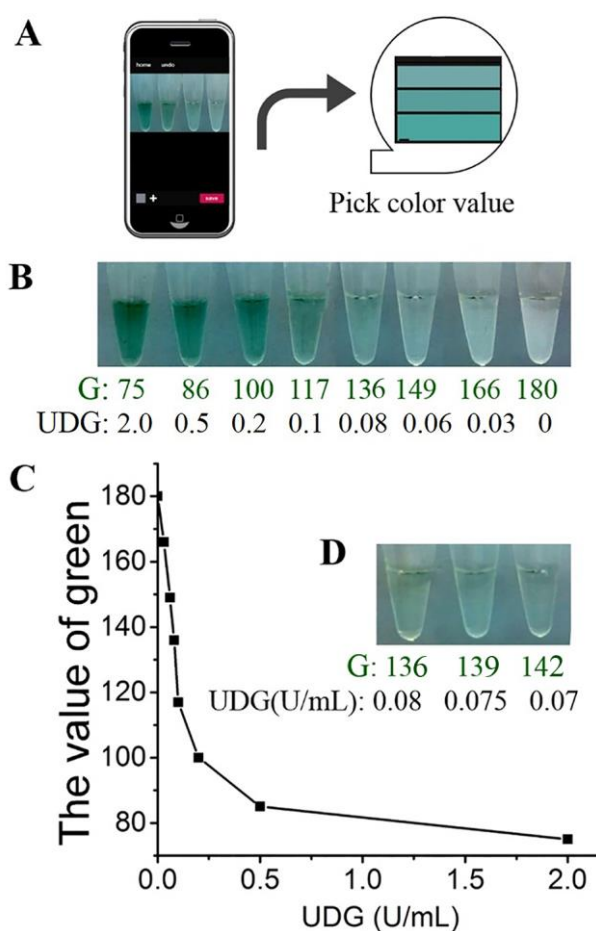


**Fig. 4**(A) Readout color value by smartphone. (B) Value of green picked by smartphone under different UDG concentrations. (C) The relationship between the UDG concentration and the value of

green. (D) Three similar concentrations of UDG were analyzed with RGB image profiling method.

In addition, fluorescent method is an alternative approach to the visible analysis of UDG, as some fluorescent substances can emit visible light under the excitation of a certain wavelength of light. Thioflavin T (ThT) is a kind of fluorescent substance that is recently demonstrated to be highly specific for G-quadruplex among other DNA forms, and the binding with G-quadruplex causes a high emission enhancement at 487 nm, compared to its weakly fluorescence in the free state. Herein, we utilize ThT as fluorescent probe to probe UDG activities. Once uracil in the La<sub>1</sub> was excised by UDG, ThT can impel the hybrid duplex to unwind and to form the G-quadruplex/ThT complex (Scheme 1, path E). Compared with G4-DNAzyme, ThT combining with G-quadruplex can display sharply enhanced signal without any assistance of other substances. Fig. 5A shows that the fluorescence emission enhance with the increasing UGD concentration under the UV lamp. Fig.5B shows the fluorescence emission at 487 nm with different concentration of UDG. As the UDG concentration increases, the fluorescence orderly enhances correspondingly. As the concentration ranging from 0.01 to 0.2 U/mL, the UDG has a good linear response toward the fluorescence intensity. Its detection limit is about 0.01 U/mL, which is similar to the detection result based on the DNAzyme platform. The linear equation of the fluorescence experiment is  $FI = 7.01 \times 10^5 C_{UDG} + 1.72 \times 10^5$ . This method exhibits an apparent improvement in the detection limit compared with fluorescence labeling methods without a signal amplifier.

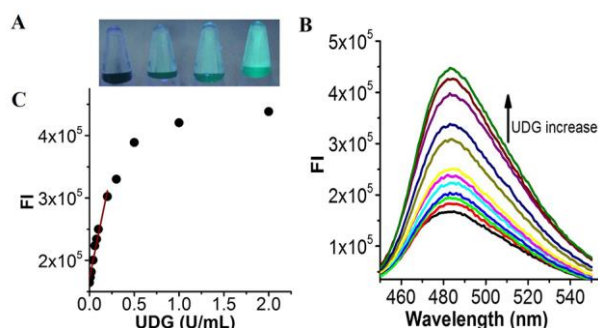


**Fig. 5(A)** Photography of the fluorescence intensity of TdT-generated G-quadruplexes under the UV lamp (from left to right, Lb4, La1 and Lb4 without UDG, La1 and Lb4 with 0.2 U/mL UDG, La1 and Lb4 with 2 U/mL UDG). **(B)** The fluorescence emission variation versus different concentration of UDG. **(C)** The fluorescence intensity of G-quadruplex/ThT at 485 nm was plotted as a function of the UDG concentration.

The utility of such G-quadruplex-based assay for screening potential UDG inhibitors were also studied. UGI was selected as a model inhibitor for this study. UGI which is produced by the bacteriophage PBS1 can form an extremely specific and exclusively stable complex with UDG with a 1:1 stoichiometry.<sup>27</sup> Once interacting with UGI and forming a stable complex, UDG loses its physiological function and can no longer excise the uracils from DNA strands. In the UDG inhibitor experiment, UDG was mixed with UGI according to the molar ratio of 1:1 at first, then the

follow-up steps are the same as the aforementioned. The results presented in Fig. 6A are according with our assumption excellently. When the UDG activity is suppressed by UGI, it cannot excise the uracil from the DNA strand, and the guanine-rich strand cannot break off from the heteroduplex. As a result, no relevant signal was detected. These results also demonstrate that the proposed method can be used to screen UDG inhibitors simply and rapidly, which may have potential biological applications. Furthermore, the selectivity of this UDG activity detection platform was also evaluated with three proteins. Nucleoproteins DpnI restriction enzyme, another BER enzyme human alkyl adenine DNA glycosylase (hAAG) and a nonspecific protein bovine serum albumin (BSA) were chosen as the control. As Fig. 6B shown, no evident signal was detected among the three proteins compared with the background. Therefore, the proposed strategy shows high selectivity for UDG.

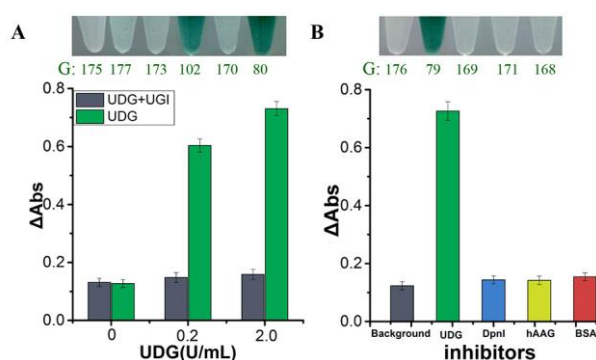


**Fig. 6** (A) The RGB analysis applied in the inhibitor research (upper). Absorbance change of DNazyme (lower) with different concentration of UDG (the green bars) and UDG is mixed with UGI (the yellow green bars). (B) The RGB analysis applied in the selectivity study (upper). Absorbance change (lower) with 2 U/mL UDG (the green bar), 2 U/mL DpnI (the blue bar), 2 U/mL hAAG (the yellow bar), 1 mg/mL BSA (the red bar).

## Conclusion

In summary, for the purpose of exploiting a simple and visible strategy to achieve an effective analysis of BER, we developed a target-activated G-quadruplex strategy for colorimetric detection of UDG activity. Our G-quadruplex-based assay possesses several advantages. First of all, we provide a BER assay without requirement of complicated instruments which is close to the ordinary people and catering to the development of the portable diagnosis. Second, the assay of BER can be simply visualized by naked-eyes. Third, using a smartphone App to read out the RGB data of the samples, we can easily reason out the UDG concentration, providing a new vision for the portable assay strategy. Fourth, the labor-intensive modification of DNA probes is avoided in this method, which is facile, cost-effective and appropriate suitable in resource-limited condition. Finally, this method is highly sensitive with a low detection limit without the assistance of enzyme. Furthermore, we have demonstrated that this strategy could be potentially employed as a screening platform for UDG inhibitors. Therefore, we envisage that this simple and visible strategy can be expanded to other biological molecular assays and the screening of protease

1  
2  
3 inhibitors.  
4  
5

### 6 **Acknowledgements**

7 This work was financially supported by the National Natural Science Foundation of  
8 China (Nos. 21475037, 21305037 and 20110041) and the Fundamental Research Funds  
9 for the Central Universities.  
10  
11

### 12 **References**

- 13 1. T. Lindahl, *Nature*, 1993, 362, 709-715.
- 14 2. G. G. Xu, M. Herzig, V. Rotrekl and C. A. Walter, *Mech. Ageing Dev.* 2008,129, 366-382.
- 15 3. G. Slupphaug, C. D. Mol, B. Kavli, A. S. Arvai, H. E. Krokan and J. A. Tainer, *Nature*, 1996,  
16 384, 87-92.
- 17 4. A. Vem, P. Mazzarello, G. Biamonti, S. Spadari, and F. Focher, *Nucleic Acids Res.*, 1990, 18,  
18 5775-5780.
- 19 5. L. A. Barouch, D. Q. Gao, L. Chen, K. L. Miller, W. H. Xu, A. C. Phan, M.M. Kittleson, K. M.  
20 Minhas, D. E. Berkowitz, C. M. Wei and J. M. Hare, *Circulation Research*, 2006, 98, 119-124.
- 21 6. C. F. Li, J. X. Feng and H. X. Ju, *Analyst*, 2015, 140, 230-235.
- 22 7. C. K. Anders, E. P. Winer, J. M. Ford, R. Dent, D. P. Silver, G.W. Sledge, L. A. Carey, *Clin.*  
23 *Cancer Res.*, 2010, 16, 4702-4710.
- 24 8. J. Tchou, H. Kasai, S. Shibutani, M. H. Chung, J. Laval, A. P. Grollman, and S. Nishimura,  
25 *Proc. Natl. Acad. Sci.*, 1991, 88, 4690-4694.
- 26 9. H. Krokan, and C. U. Wittwer, *Nucleic Acids Res.*, 1981, 9, 2599-2613.
- 27 10. A. A. Ischenko, and M. K. Sapparbaev, *Nature*, 2002, 415, 183-187.
- 28 11. L. Zhang, J. Zhao, J. Jiang and R. Yu, *Chem. Commun.*, 2012, 48, 8820-8822.
- 29 12. D. Hu, Z. Huang, F. Pu, J. Ren and X. Qu, *Chem.-Eur. J.*, 2011, 17, 1635-1641.
- 30 13. Y. Xiang, Y. Lu, *Anal. Chem.*, 2012, 84, 9981-9987.
- 31 14. X. J. Liu, M. Q. Chen, T. Hou, X. Z. Wang, S. F. Liu and F. Li, *Electrochim. Acta.*, 2013, 113,  
32 514-518.
- 33 15. X. J. Liu, M. Q. Chen, T. Hou, X. Z. Wang, S. F. Liu and F. Li, *Biosens. Bioelectron.*, 2014,  
34 54, 598-602.
- 35 16. D. M. Zhou, Q. Xi, M. F. Liang, C. H. Chen, L. J. Tang and J. H. Jiang, *Biosens. Bioelectron.*,  
36 2013, 41, 359-365.
- 37 17. I. Willner, B. Shlyahovsky, M. Zayats, and B. Willner, *Chem. Soc. Rev.*, 2008, 37, 1153-1165.
- 38 18. W. Li, Z. L. Liu, H. Lin, J. H. Chen, X. H. Xiu, Z. Nie, S. Z. Yao, *Anal. Chem.*, 2010, 82,  
39 1935-1941.
- 40 19. H. W. Lin and K. S. Suslick, *J. Am. Chem. Soc.*, 2010, 132, 15519-15521.
- 41 20. C. C. Chiao, J. K. Wickiser, J. J. Allen, B. Genter, and R. T. Hanlon, *Proc. Natl. Acad. Sci.*,  
42 2011, 108, 9148-9153.
- 43 21. Y. K. Lee, S. Kim, J. W. Oh, and J. M. Nam, *J. Am. Chem. Soc.*, 2014, 136, 4081-4088.
- 44 22. J. Mohanty, N. Barooah, V. Dhamodharan, S. Harikrishna, P. I. Pradeepkumar, and A. C.  
45 Bhasikuttan, *J. Am. Chem. Soc.*, 2013, 135, 367-376.
- 46 23. K. H. Leung, H. Z. He, V. P. Y. Ma, H. J. Zhong, D. S. H. Chan, J. Zhou, J. L. Mergny, C. H.  
47 Leung and D. L. Ma, *Chem. Commun.*, 2013, 49, 5630-5632.
- 48 24. B. Liu, X. H. Yang, W. H. Tan, H. M. Li, H. X. Tang and K. M. Wang, *Anal. Biochem.*, 2007,  
49  
50  
51  
52  
53  
54  
55  
56  
57  
58  
59  
60

1  
2  
3  
4 366, 237-243.

5 25. C. Li, Y. Long, B. Liu, D. Xiang and H. Z. Zhu. *Anal. Chim. Acta*, 2014, 819, 71-77.

6 26. S. Seidi, M. Rezaadeh, Y. Yamini, N. Zamani and S. Esmaili, *Analyst*, 2014, 139,  
7 5531-5537.

8 27. A. Hakonen, J. E. Beves and N. Strömberg, *Analyst*, 2014, 139, 3524-3527.

9 28. S. E. Bennett and D. W. Mosbaugh, *J. Biol. Chem.*, 1992, 267, 22512-22521.  
10  
11  
12  
13  
14  
15  
16  
17  
18  
19  
20  
21  
22  
23  
24  
25  
26  
27  
28  
29  
30  
31  
32  
33  
34  
35  
36  
37  
38  
39  
40  
41  
42  
43  
44  
45  
46  
47  
48  
49  
50  
51  
52  
53  
54  
55  
56  
57  
58  
59  
60